



**HAL**  
open science

# SCALE-CONTROLLED SULCAL DEPTH ESTIMATION

Maxime Dieudonne, Guillaume Auzias, Julien Lefèvre

► **To cite this version:**

Maxime Dieudonne, Guillaume Auzias, Julien Lefèvre. SCALE-CONTROLLED SULCAL DEPTH ESTIMATION. IEEE International Symposium on Biomedical Imaging (ISBI 2024), May 2024, Athens, Greece. hal-04608745

**HAL Id: hal-04608745**

**<https://hal.science/hal-04608745v1>**

Submitted on 11 Jun 2024

**HAL** is a multi-disciplinary open access archive for the deposit and dissemination of scientific research documents, whether they are published or not. The documents may come from teaching and research institutions in France or abroad, or from public or private research centers.

L'archive ouverte pluridisciplinaire **HAL**, est destinée au dépôt et à la diffusion de documents scientifiques de niveau recherche, publiés ou non, émanant des établissements d'enseignement et de recherche français ou étrangers, des laboratoires publics ou privés.

Copyright

# SCALE-CONTROLLED SULCAL DEPTH ESTIMATION

*M. Dieudonné, G. Auzias, J. Lefèvre*

Aix-Marseille Université, CNRS, Institut de Neurosciences de la Timone, Marseilles, France

## ABSTRACT

The complex brain morphology emerges from intricate growth and folding processes during development. Sulcal depth is a shape descriptor particularly relevant to characterize brain development and variations, but the potential influence of global brain size is not controlled in existing estimation techniques. In this work, we address this issue by introducing a theoretical framework allowing to explicitly control for the influence of isometric scaling on sulcal depth measured at each brain location. We provide both formal and experimental demonstrations of the advantages compared to the most popular method from the literature.

**Index Terms**— MRI, Brain, Cortex, surface, morphometry

## 1. INTRODUCTION

The human brain cortex has a labyrinthine geometry composed of ridges and valleys at adult age. This geometry is the result of complex biological processes [1]. The variations in brain shape across individuals have been extensively described in the literature [2], with the dissociation of two components that are not independent: global size and degree of gyrification. The potential influence of variations in global brain size on morphometry descriptors computed locally is however largely ignored.

One key descriptor of the morphology of the cortical surface is sulcal depth. There is growing evidence that sulcal depth is particularly relevant for characterizing brain development. Sulcal depth has been used to describe the spatio-temporal evolution of brain folding in human fetuses and newborns [3], between birth and adulthood [4] as well as in other gyrencephalic species [5]. Recent studies suggest that sulcal depth measures in fetuses provides prognostic value of later cognitive development [6], and is instrumental to detect neuro-developmental malformations [7].

The most intuitive way to define the sulcal depth of each point of the cortical surface is to compute the distance between the spatial location of the point of interest and the closest point on the 'convex hull' of the brain. But already with this intuitive definition, two main ambiguities emerge when moving from concept to implementation: First, computing the 'convex hull' that implicitly corresponds to the 0-level

(or reference-level) for the depth measure is not trivial. Indeed, a mathematically correct definition of the convex hull of the cortical surface would not follow closely most concave regions such as the internal temporal region, resulting in a local over estimation of the sulcal depth. The implementations of this 'convex hull' thus rely on a proxy consisting in applying a morphological closing of the volumetric segmentation mask of the cortex, which is efficient but question the potential influence between the size of the closing operator and the global size of the brain of interest. Second, there is no unique way to compute the distance to the convex hull and several approaches have been proposed. We refer the readers interested in a detailed comparison across these types of approaches to [8] which provides both qualitative and quantitative comparisons.

Another strategy for estimating sulcal depth without considering the convex hull has been introduced in [9]. We refer to this method as SULC in the following. SULC estimates the sulcal depth as the distance between the initial mesh and an inflated version of the considered mesh. The distance is computed through the iterative inflation process. A critical parameter here is the number of iterations allowing to inflate the original brain. In the two available implementations of SULC from the widely used freesurfer software <sup>1</sup> or the dHCP pipeline <sup>2</sup>, the number of iterations was set based on experiments on adult brains only, without considering the size of the brain.

Another approach introduced in [10] proposes to estimate sulcal depth from the mean curvature of the surface: the depth potential (DPF) is defined as the solution  $D$  of the following regularized screened Poisson equation:

$$(-\Delta_M + \alpha I)D = K \quad (1)$$

where  $\Delta_M$  is the Laplace-Beltrami operator of the surface  $M$  (negative operator),  $I$  is the identity operator,  $K$  the mean curvature of  $M$  and  $\alpha$  a regularization parameter. The only parameter  $\alpha$  was set based on visual assessment.

To the best of our knowledge, all the sulcal depth estimation techniques from the literature have been designed and evaluated on adult brains only, without considering the potential influence of global brain size. The interaction between

<sup>1</sup><https://surfer.nmr.mgh.harvard.edu/>

<sup>2</sup><https://github.com/BioMedIA/dhcp-structural-pipeline>

cortical global brain size and cortical folding magnitude is never discussed explicitly. There is clear need to explicitly investigate the crucial problem of the intricate variations in global brain size and folding. In the present work, we address this question by proposing a formalization of the problem, introducing a scale-invariant sulcal depth estimation method, and providing theoretical and experimental demonstration of its advantages compared to the most widely used method.

## 2. METHODS

### 2.1. Formal problem statement

Let  $M$  be any surface embedded in  $\mathbb{R}^3$  and approximated by a triangular mesh with  $p$  vertices. We consider a family of scalar functions depending both of a surface  $M$  and parameters  $\chi$ . Formally

$$D_M(\cdot, \chi) : p \in M \subset \mathbb{R}^3 \longrightarrow D_M(p, \chi) \in \mathbb{R} \quad (2)$$

This very general framework systematically involves parameters  $\chi$  allowing to adapt the underlying algorithm e.g. to the spatial discretisation of the ambient space (size of the voxels) or of the mesh (size of the triangles). Taking as an example the sulcal depth for a given surface  $M$ , the collection of parametric functions  $\chi \rightarrow D_M(\cdot, \chi)$  represents all the possible settings to compute an estimation of the sulcal depth on  $M$ . For instance, in the case of a method based on the distance to the convex hull,  $\chi$  consists of all possible settings of the structuring elements in the morphological closing of the volumetric segmentation of the brain used to compute the convex hull. In the case of the SULC method (described above),  $\chi$  consists of all possible settings of the parameters that control for the inflation of the mesh.

We now define the **scaling** between two surfaces  $M_1$  and  $M_2$  as a linear transformation defined by the parameter  $s > 0$  where coordinates of  $M_2$  correspond to the multiplication of the coordinates of  $M_1$  by the factor  $s$ . In particular lengths have been multiplied by  $s > 0$ . We note this scaling relationship between the two surfaces as  $M_2 := sM_1$ . And we now formalize the influence of the scaling of factor  $s$  on a family of functions  $D_M(\cdot, \chi)$ .

**Definition 1.** *We state that a family of functions  $D_M(\cdot, \chi)$  is **scale invariant** if, for  $s > 0$  and  $M_2 := sM_1$ , there exists a transformation in the space of parameters,  $f(s, \chi)$  such as:*

$$D_{M_1}(\cdot, \chi) = D_{M_2}(\cdot, f(s, \chi)) \quad (3)$$

This formula makes it explicit that the parameters have to be adapted when the scale of the surface changes. In other words, it is expected that when considering functions  $D_M(\cdot, \chi)$  which were designed to estimate quantities that are related to physical units, such as depth, thickness and even brain activity (related to electro-magnetism or blood flow) the

invariance to scale is impossible without appropriate tuning of its parameters  $\chi$ .

Now, as mentioned in the introduction, scale invariance is not a desired feature in applications to cortical surfaces. Indeed, larger brains are also more folded, which induces that most functions measuring a biological process defined on the cortex are expected to be impacted by the size of the brain. We therefore introduce the notion of control on the influence of the scale as follows:

**Definition 2.** *We state that a family of functions  $D$ , depending on parameters  $\chi$  is **scale controlled** if for any  $s > 0$  one can find  $f(s, \chi)$  and  $d(s)$  such as  $\frac{1}{d(s)}D_{sM}(\cdot, f(\chi, s))$  is scale invariant. Which can be formulated, for a point  $p \in M$ , as:*

$$\underbrace{\frac{1}{d(s)}}_{\text{normalisation}} D_{sM}(p, \underbrace{f(s, \chi)}_{\text{adaptation}}) = \frac{1}{d(1)} D_M(p, f(1, \chi)) \quad (4)$$

This equation makes a formal link between the estimations from two surfaces  $M$  and  $sM$ : for any method  $D$  satisfying this equation, the estimation  $D_{sM}$  on a scaled surface is related to the estimation obtained on the original surface through two factors: a multiplicative function of  $d(s)$  called the **normalization** function and an **adaptation** function  $f$  that corresponds to an adaptation of the parameters. The normalization function corresponds to normalizing the range of the values covered across the points of each surface.

### 2.2. DPF with formal control on the scale of the surface

We now consider the application of the formalism provided above to a specific type of functions: sulcal depth. The surface  $M$  corresponds to the interface between the gray and white matter of the brain. The scaling factor between any two brain  $s$  is estimated as the ratio of the cubic root of the volumes considered, i.e.  $s = (V_2/V_1)^{1/3}$ .

We now consider more precisely the depth potential function (DPF) as our method of interest. As mentioned in the introduction, the DPF has been defined in [10] as the solution  $D$  of Eq.1. Regarding our previous definitions, the DPF is a family of functions with only one parameter  $\alpha$ . In the following we denote it as  $D_M(\cdot, \alpha)$ .

**Theorem 1.** *The DPF is scale-controlled and we have the explicit formula*

$$f(s, \alpha) = s^{-2}\alpha \text{ and } d(s) = s \quad (5)$$

*Proof.* We denote  $M_2$  the surface obtained by applying a scaling of parameter  $s$  to the surface  $M_1$ , i.e.  $M_2 := sM_1$ .

We recall the intrinsic property of the Laplace-Beltrami operator and mean curvature:

$$\Delta_{M_2} = s^{-2}\Delta_{M_1} \quad K_{M_2} = s^{-1}K_{M_1} \quad (6)$$

Equation 1 on  $M_2$  with a parameter  $\alpha_2$  can be transformed into an equation on  $M_1$ :

$$-\Delta_{M_2} D_{M_2} + \alpha_2 D_{M_2} = K_{M_2} \quad (7)$$

$$\Leftrightarrow -\Delta_{M_1} D_{M_2} + \alpha_2 s^2 D_{M_2} = s K_{M_1} \quad (8)$$

Calling  $\alpha = \alpha_2 s^2$ , the previous equation can be written as

$$-\Delta_{M_1} (s^{-1} D_{M_2}) + \alpha (s^{-1} D_{M_2}) = K_{M_1} \quad (9)$$

The previous equation tells us that  $s^{-1} D_{M_2}(\cdot, \alpha_2)$  is a solution of the Poisson equation on  $M_1$  with parameter  $\alpha$ . Since Poisson equation admits a unique solution, we conclude that :

$$s^{-1} D_{M_2}(\cdot, s^{-2} \alpha) = D_{M_1}(\cdot, \alpha) \quad (10)$$

So that Eq.4 is satisfied and we get that  $D$  is scale controlled.  $\square$

We can now define a new sulcal depth estimation derived from the DPF:

**Definition 3.** We consider a reference surface  $M_0$  and a parameter  $\alpha > 0$ . We define  $s = (V_M/V_0)^{1/3}$  where  $V_0$  and  $V_M$  are the volumes of surfaces  $M_0$  and  $M$ . We call  $DPF^*$  the scale invariant function satisfying:

$$DPF_M^*(\cdot, \alpha) = s^{-1} DPF_{M_0}^*(\cdot, \alpha s^{-2}) \quad (11)$$

We can examine two situations:

- a) In the ideal case where  $M$  is a scaled version of the reference surface  $M_0$ ,  $DPF_M^*$  will be identically equal to  $DPF_{M_0}^*$ .
- b) In real world applications, two cortical surfaces  $M$  and  $M_0$  are never related by a simple scaling, but by a relationship involving a global scaling but also complex local deformations. In that case, we get  $DPF_M^* \neq DPF_{M_0}^*$ , but  $DPF_M^*$  can be considered as an approximation of  $DPF_{M_0}^*$  in which we compensate for the influence of global scaling.

### 2.3. Setting of the parameter $\alpha$ for the reference surface

We have shown above how to adapt the  $\alpha$  parameter as a function of the sizes of a meshes  $M$  and  $M_0$ . We now need to define its value so that it is adapted to the mesh  $M_0$ . It has been shown in [10] that solving the Poisson equation is equivalent to a low-pass curvature filtering. The transfer function is expressed as:

$$D_i = \frac{1}{\alpha + \lambda_i} K_i \quad (12)$$

with  $D_i$  and  $K_i$  the Fourier coefficients of the depth and curvature expressed in the eigenvector basis of the Laplace-Beltrami Operator. As described in [11],  $\lambda_i$  are the eigenvalues that we can interpret as spatial frequencies  $f_i$  and

consequently with a spatial wavelength  $L_i$  according to the relations

$$f_i = \frac{1}{L_i} = \frac{\sqrt{\lambda_i}}{2\pi} \quad (13)$$

by setting  $\alpha = 500$  we obtain a frequency of mid-amplitude of our transfer function  $f_i = \sqrt{500}/(2\pi)$  or  $L_i = 28$  mm which corresponds to the order of magnitude of the geodesic width of a sulci on an average brain. We confirmed the relevance of this setting by visual inspection of *several brains with different degree of folding and global size*. Note that contrary to SULC and other sulcal depth estimation methods, the setting of  $\alpha$  of  $DPF^*$  is thus appropriate for brains of various size and not only for adult brains.

## 3. EXPERIMENTS AND RESULTS

In a first experiment, we provide empirical evidence that our method is scale-controlled, and show quantitatively that it is not the case for SULC. In the second experiment, we demonstrate the practical relevance of our approach by exploring one of the many potential applications: sulcal basins segmentation across a large population of brains with strong variations in brain size and folding.

We aggregated a collection of cortical surfaces showing strong variations in brain size and magnitude of cortical folding. To do so, we selected individual data from two publicly available datasets: 1) The dHCP dataset consists of MRI data from 783 newborn babies covering the ages from 26 to 45 weeks post-conception. The segmentation and surface extraction tools are detailed in [12]. 2) The KKI (Kennedy Krieger Institute, [13]) dataset consists of high quality MRI data from 21 healthy adults. We downloaded the raw MRI data and used the recon-all pipeline from freesurfer 6.0 to extract the cortical surfaces.

### Experiment 1 : simulations

In this experiment, we investigate the influence of simulated scaling on SULC and confirm empirically the invariance of  $DPF^*$ . The results from this experiments are reported on Fig.1. We select a cortical mesh from a young subject from the dHCP (29GW) and apply different scaling of coefficients between 1 and 5 that results in 5 meshes with same folding pattern but different sizes. We then compute the SULC and  $DPF^*$  sulcal depth on these 5 surfaces. In order to characterize the influence of the scaling on the estimated sulcal depth, we compute the linear regression across all the vertices of the mesh between the depth estimated on the scaled surface and the depth estimated on the original surface (scale=1). If the method is scale invariant, the correlation coefficient should be equal to 1 and the slope of the regression line should also be equal to 1. This is what we observe for the  $DPF^*$ , as expected from its formal definition. If the global scaling affects the estimated sulcal depth, then the regression line might deviate from  $y = x$ , and/or the correlation coefficient might be lower than 1. We observe such deviations for the SULC.

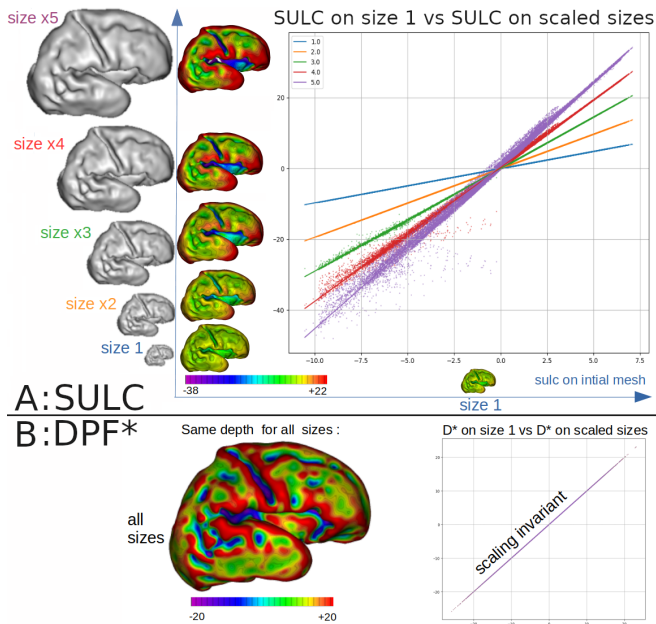


**Fig. 1. A.** Left: Sulcal depth estimation obtained using SULC for the different scalings. When the scaling increases, the sulcal depth seems not biologically relevant in large concave regions such as the frontal and temporal lobes (in red). Right: Linear regressions for the different scalings. Both the slope and the correlation values depend on the scaling factor. **B.** The sulcal depth maps generated using the  $DPF^*$  method on the scaled meshes are independent from the size of the mesh and thus identical.

### Experiment 2 : real data

In this experiment, we aim to compare the methods in a real world application. As suggested in [14], the progressive folding of the brain during maturation can be quantified by computing the proportion of sulci according to the whole brain size. In this experiment, we assess whether the sulci can be effectively segmented by simply applying a threshold to the individual sulcal depth maps. To do so, we select 94 subjects (73 from dHCP, 21 from KKI) covering the range of size of the postnatal human brain development, with volumes varying from  $50000mm^3$  to  $300000mm^3$ . We compute SULC and  $DPF^*$  for each individual independently. We then dissociate sulci from gyri by applying a common threshold to all the sulcal depth estimation obtained from each of the two methods. The threshold value was computed for each method as the median across all the estimations from all the subjects. We then compute for each brain the ratio of surface area corresponding to sulci and gyri and obtain the percentage of surface corresponding to sulci. We also compute for each brain the gyrification index which is defined as the ratio between the area of the folded mesh and the area of its convex hull. The gyrification index is thus a measure of the degree of folding of a brain. The results from this experiment are reported

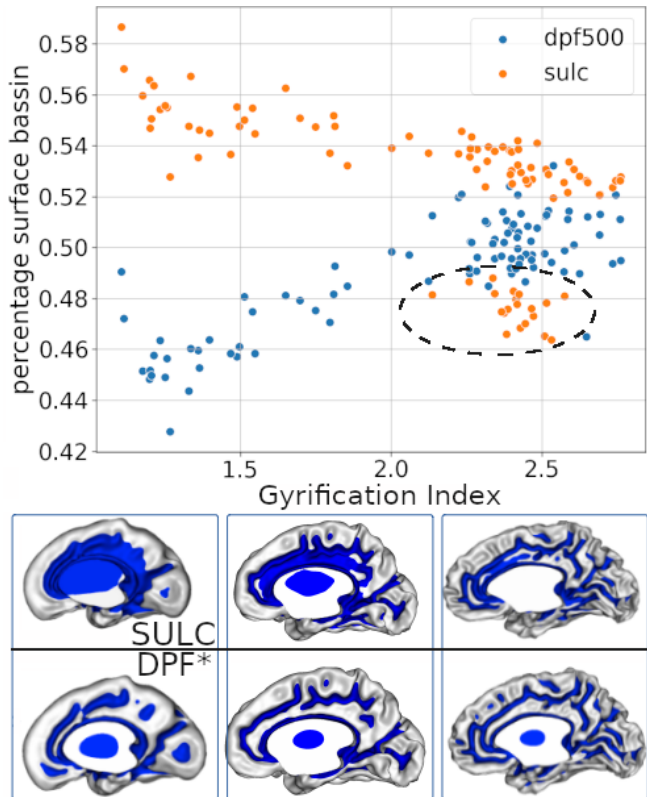


**Fig. 2. Top.** Scatter plot of the percentage of sulci as a function of the level of gyrification. **Bottom.** Thresholded depth maps obtained for 3 brains with different degree of folding. With  $DPF^*$ , the concave regions in blue correspond to sulci across all brains. It is not the case for SULC.

on Fig.2. With the  $DPF^*$ , we observe an increase of the percentage of sulci with higher gyrification index, as expected. The confounding influence of global scale on SULC induces an inverted relationship between the percentage of sulci and gyrification index. In addition, contrary to  $DPF^*$  for which the relationship between the two measures is continuous, we observe two separated clusters with SULC. The percentage of sulci obtained for adult brains (located in the ellipse) is lower than for younger brains that are visually less folded. The estimated sulcal depth from SULC are not biologically relevant in this experiment.

## 4. CONCLUSION

We introduce a new sulcal depth estimation technique with a formal control on the influence of the global size of the brain. Our experiments on simulations and real data show that our technique addresses the limitations of the reference method from the literature.

## 5. COMPLIANCE WITH ETHICAL STANDARDS

This research study was conducted retrospectively using human subject data made available in open access by the dHCP (<http://www.developingconnectome.org>) and the KKI (Kennedy Krieger Institute, [13]). Both studies were approved by their respective institutional review board.

## 6. ACKNOWLEDGMENTS

Data were provided by the developing Human Connectome Project, KCL-Imperial-Oxford Consortium funded by the European Research Council under the European Union Seventh Framework Programme (FP/2007-2013) / ERC Grant Agreement no. [319456]. We thank the Agence National pour la Recherche for supporting this study under the Sulcal Grid project (ANR-19-CE45-0014) and the Eranet project (ANR-21-NEU2-0005). The authors have no relevant financial or non-financial interests to disclose.

## 7. REFERENCES

- [1] I. Kostović, G. Sedmak, and M. Judaš, “Neural histology and neurogenesis of the human fetal and infant brain,” *NeuroImage*, vol. 188, no. December 2018, pp. 743–773, Mar. 2019.
- [2] P. K. Reardon, Jakob Seidlitz, Simon Vandekar, Siyuan Liu, Raihaan Patel, Min Tae M. Park, Aaron Alexander-Bloch, Liv S. Clasen, Jonathan D. Blumenthal, Francois M. Lalonde, Jay N. Giedd, Ruben C. Gur, Raquel E. Gur, Jason P. Lerch, M. Mallar Chakravarty, Theodore D. Satterthwaite, Russell T. Shinohara, and Armin Raznahan, “Normative brain size variation and brain shape diversity in humans,” *Science*, vol. 360, no. 6394, pp. 1222–1227, 2018.
- [3] Hyuk Jin Yun, Lana Vasung, Tomo Tarui, Caitlin K Rollins, Cynthia M Ortnau, P Ellen Grant, and K. Im, “Temporal Patterns of Emergence and Spatial Distribution of Sulcal Pits During Fetal Life,” *Cerebral Cortex*, pp. 1–12, 2020.
- [4] Jason Hill, Terrie E Inder, Jeffrey J Neil, Donna L. Dierker, John W Harwell, and David C. Van Essen, “Similar patterns of cortical expansion during human development and evolution -Supporting Information,” *Proceedings of the National Academy of Sciences of the United States of America*, vol. 107, no. 8, pp. 40–42, July 2010.
- [5] Andrew K Knutsen, Christopher D. Kroenke, Yulin V Chang, Larry a Taber, and Philip V. Bayly, “Spatial and temporal variations of cortical growth during gyrogenesis in the developing ferret brain.,” *Cerebral cortex (New York, N.Y. : 1991)*, vol. 23, no. 2, pp. 488–98, Mar. 2013.
- [6] Lisa Bartha-Doering, Kathrin Kollndorfer, Ernst Schwartz, Florian Ph S. Fischmeister, and et al., “Fetal temporal sulcus depth asymmetry has prognostic value for language development,” *Communications Biology*, vol. 6, no. 1, pp. 1–9, Jan. 2023, Number: 1 Publisher: Nature Publishing Group.
- [7] L. Brun, G. Auzias, Marine Viellard, N. Villeneuve, and et al., “Localized Misfolding Within Broca’s Area as a Distinctive Feature of Autistic Disorder,” *Biological Psychiatry: Cognitive Neuroscience and Neuroimaging*, vol. 1, no. 2, pp. 160–168, Mar. 2016.
- [8] Hyuk Jin Yun, K. Im, Jin-Ju Yang, Uicheul Yoon, and Jong-Min Lee, “Automated sulcal depth measurement on cortical surface reflecting geometrical properties of sulci.,” *PLoS one*, vol. 8, no. 2, pp. e55977, Jan. 2013.
- [9] B. Fischl, Martin I Sereno, and A. M. Dale, “Cortical surface-based analysis. II: Inflation, flattening, and a surface-based coordinate system.,” *NeuroImage*, vol. 9, no. 2, pp. 195–207, Feb. 1999, Publisher: Elsevier.
- [10] Maxime Boucher, Sue Whitesides, and Alan C Evans, “Depth potential function for folding pattern representation, registration and analysis,” *Medical image analysis*, vol. 13, no. 2, pp. 203–14, Apr. 2009, Publisher: Elsevier B.V.
- [11] D. Germanaud, J. Lefèvre, R. Toro, C. Fischer, J. Dubois, L. Hertz-Pannier, and J.-F. Mangin, “Larger is twistier: Spectral analysis of gyrification (SPANGY) applied to adult brain size polymorphism.,” *NeuroImage*, vol. 63, no. 3, pp. 1257–72, Nov. 2012, Publisher: Elsevier Inc.
- [12] A. Makropoulos, Emma C Robinson, Andreas Schuh, and et al., “The developing human connectome project: A minimal processing pipeline for neonatal cortical surface reconstruction,” *NeuroImage*, vol. 173, pp. 88–112, June 2018.
- [13] Bennett A. Landman, Alan J. Huang, Aliya Gifford, and et al., “Multi-parametric neuroimaging reproducibility: A 3-T resource study,” *NeuroImage*, vol. 54, no. 4, pp. 2854–2866, Feb. 2011, ISBN: 4109176166 Publisher: Elsevier Inc.
- [14] J. Dubois, M. Benders, C Borradori-Tolsa, A. Cachia, F. Lazeyras, R. Ha-Vinh Leuchter, and et al., “Primary cortical folding in the human newborn: an early marker of later functional development,” *Brain*, vol. 131, no. 8, pp. 2028–41, Aug. 2008.